

Sulfasalazine as a Corrosion Inhibitor on Carbon Steel Metal Surfaces in Acidic Media Using the Hydrogen Evolution Method: Experimental and Theoretical Studies

Hadi Thamer Obaid^{1,2}, Muthanna Mahmood Mutar^{2,3}, and Safaa Hussein Ali^{4*}

¹Department of Medical Physics, College of Applied Medical Sciences, Al-Shatrah University, Thi-Qar 64007, Iraq

²College of Science, Uruk University, Baghdad 10075, Iraq

³Education Directorate of Thi-Qar, Ministry of Education, Thi-Qar 64001, Iraq

⁴Continuous Learning Center, Al-Shatrah University, Al-Shatrah, Thi-Qar 64007, Iraq

* **Corresponding author:**

tel: +964-7808901830

email: safaa.ali@shu.edu.iq

Received: May 2, 2024

Accepted: September 6, 2024

DOI: 10.22146/ijc.95852

Abstract: Current study designed to explore the anti-corrosion effect of 2-hydroxy-5-*[(E)-[4-(pyridin-2ylsulfamoyl)phenyl]diazenyl]* benzoic acid (sulfasalazine, SSZ) on carbon steel. 1 M of HCl solution used as an aggressive medium. The corrosion process was significantly inhibited by SSZ using simple, direct and accurate method (hydrogen evolution) to measure corrosion inhibition process. The results showed that the corrosion inhibition efficiency increased with increasing the inhibitor SSZ concentration. Three different concentrations of the inhibitor SSZ (0.1×10^{-3} , 0.5×10^{-3} , and 1.0×10^{-3} M) were used in the corrosion experiment. Results showed a maximum inhibition efficiency (89.74%) achieved at the concentration of 1×10^{-3} M and the temperature of 308 K. The calculations of the hydrogen evolution method showed that the investigated SSZ acted as a mixed-type inhibitor. Adsorption of SSZ on the carbon steel surface obeys the Langmuir adsorption isotherm. The quantitative chemical parameters were calculated using density functional theory (DFT). In addition, full geometry optimizations were performed using DFT with B3LYP. The correlation between the theoretical and experimental results is discussed. The theoretical and experimental studies showed that SSZ is a good inhibitor as the maximum anti-corrosion activity was achieved at the highest concentration of the SSZ (1×10^{-3} M), and the lowest temperature used in the experiment.

Keywords: corrosion inhibitor; carbon steel; density function theory; hydrogen evolved; sulfasalazine

■ INTRODUCTION

The corrosion of metals and alloys, along with the subsequent deterioration of their characteristics, poses a significant challenge in industry [1]. This issue is particularly concerning due to its contribution to environmental pollution [2]. In the case of the carbon steel industry, the use of acids for pickling, descaling, and cleaning exacerbates this problem [3]. As a result, scientists have been actively looking for ways to safeguard these materials and minimize their environmental impact [4]. In general, an inhibitor is a chemical used to prevent corrosion by changing the chemistry of the corrosive solution. In recent years, organic compounds such as azo,

Schiff base, and phenol have been frequently used as corrosion inhibitors [5-6]. Applying corrosion inhibitors has proven to be the most efficient and cost-effective approach for metallic protection [7-8]. These compounds form a protective layer on the surface of the metal due to their active centers, such as atoms of nitrogen (N), sulfur (S), and oxygen (O), as well as double or triple bonds [9]. These components interact with the metal surface, ultimately resulting in the creation of a protective layer [10-12]. Compounds containing π -bonds, such as azo and Schiff base [3] typically display strong inhibitive properties as a result of interactions between their π -orbitals and the metal

surface [13]. Azo compounds, which possess π -bonds and electron pairs as active centers in their structure (specifically through the N=N linkage), have emerged as highly effective and promising candidates for corrosion inhibitors [14-15].

Recently, density function theory (DFT) in quantum chemical calculations has been applied to elucidate and establish a connection between experimental results [16-17]. This approach aims to provide a comprehensive understanding of the inhibitory effects of sulfasalazine (SSZ). The reactivity of a chemical species is strongly influenced by the frontier orbital, which comprises the highest occupied molecular orbital (HOMO) and the lowest unoccupied molecular orbital (LUMO). The frontier orbital of a chemical species is considered very important in defining its reactivity [18-20]. In addition, conducting theoretical research allows for the identification of organic compounds that possess the structural features required for chemical reactions [21-23].

The primary objective of this study was to develop a corrosion inhibitor using an azo dye and assess its effectiveness in inhibiting steel corrosion in a 1.0 M HCl solution by measuring hydrogen release. Additionally, this study aimed to examine how the structural characteristics of the inhibitor impact its inhibition efficiency and to investigate the mechanism by which the inhibitor adsorbs onto the metal surface. Furthermore, this study explored the correlation between the experimental findings and the quantum chemical parameters of the developed corrosion inhibitor.

EXPERIMENTAL SECTION

Materials

All the reagents were purchased from Sigma, including SSZ (Fig. 1), analytical grade (37%) HCl and carbon steel (CS) used as supplied commercially. The composition of CS is listed in Table 1.

Instrumentation

The current study has several advantages such as cost effectiveness and the simple instruments required for hydrogen evolve collection. The following instruments

are required during the experiment; Lab Water Purification System (Thermo Fisher Scientific) and the Stuart SMP30 for melting point measurement.

Procedure

Analytical grade (37%) HCl was diluted with bidistilled water to obtain an aggressive solution of 1 M HCl. Three different concentrations (0.1×10^{-3} , 0.5×10^{-3} , and 1.0×10^{-3} M) of the inhibitor SSZ were prepared and used directly in the corrosion experiment.

RESULTS AND DISCUSSION

Hydrogen Evolved Method

Following the previously reported hydrogen evolved method [20] described in Fig. 2, This method has several advantages such as equipment availability and cost effectiveness [21]. A mild steel coupon weighing 8.0 g

Table 1. Chemical analysis (%weight) of the CS

Element	C	P	Mn	Si	Fe
Weight (%)	0.300	0.050	1.200	0.006	Rest

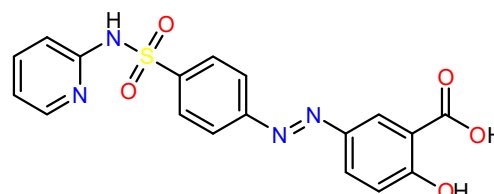


Fig 1. The chemical structure of sulfasalazine

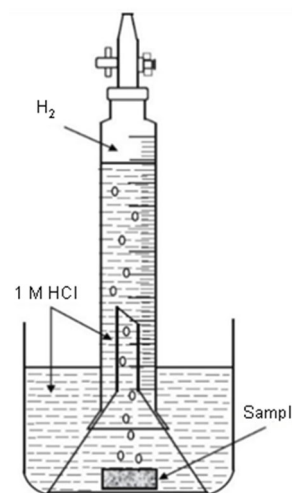


Fig 2. A schematic representation of the method used to calculate the volume of hydrogen evolved

was immersed in a 100 cm³ solution of 1 M HCl to initiate the corrosion reaction. Throughout a period of 100 min, the volume of evolved H₂ gas was measured and recorded every 60 s. The same experiment was then repeated in the presence of 5.0 mM sulfasalazine (corrosion inhibitor) in a 1 M HCl solution. The hydrogen evolution rate (R_H) was determined using Eq. (1) as specified [22];

$$R_H \text{ (cm}^3 \cdot \text{min}^{-1}) = \frac{V_1 - V_0}{t_1 - t_0} \quad (1)$$

where V_1 and V_0 are the volumes of hydrogen gas evolved (cm³) at time t_1 and t_0 (min), respectively. The inhibition efficiency (I_{HE} (%)) was calculated using Eq. (2);

$$I_{HE} \text{ (%) = } \left(1 - \frac{R_{H1}}{R_{H0}} \right) \times 100\% \quad (2)$$

where R_{H1} and R_{H0} are the hydrogen evolution rates in the presence and absence of inhibitor, respectively [23].

According to the results obtained through the hydrogen evolution method, it can be concluded as a positive relation between the inhibitor concentrations and the inhibition efficiency. The experiments were conducted with varying concentrations of SSZ (0.1×10^{-3} , 0.5×10^{-3} , and 1.0×10^{-3} M) at varied temperatures (308, 318, and 328 K) (Fig. 3(a-c)). The measured characteristics, including surface coverage (θ) and

inhibitory efficiency (%IE), are displayed in Table 2. Increasing the concentration increased the inhibition efficiency at each temperature, and the maximum recorded inhibition efficiency was 89.74% in the presence of 1×10^{-3} M SSZ at 308 K. However, there is a negative relation between the temperature and inhibition efficiency. As noticed increasing temperature above, 308 K has decreased the inhibition efficiency.

Table 2. Shows the polarization characteristics for the corrosion of carbon steel in 1 M HCl at various concentrations of SSZ and temperatures

θ	IE%	Inhibitor concentration (M)	Temperature (K)
0.0000	0.00	Blank	308
0.0000	0.00		318
0.0000	0.00		328
0.8379	83.79	0.1×10^{-3}	308
0.6609	66.09		318
0.5749	57.49		328
0.8513	85.13	0.5×10^{-3}	308
0.7000	70.00		318
0.6465	64.65		328
0.8974	89.74	1.0×10^{-3}	308
0.7980	79.80		318
0.7546	75.46		328

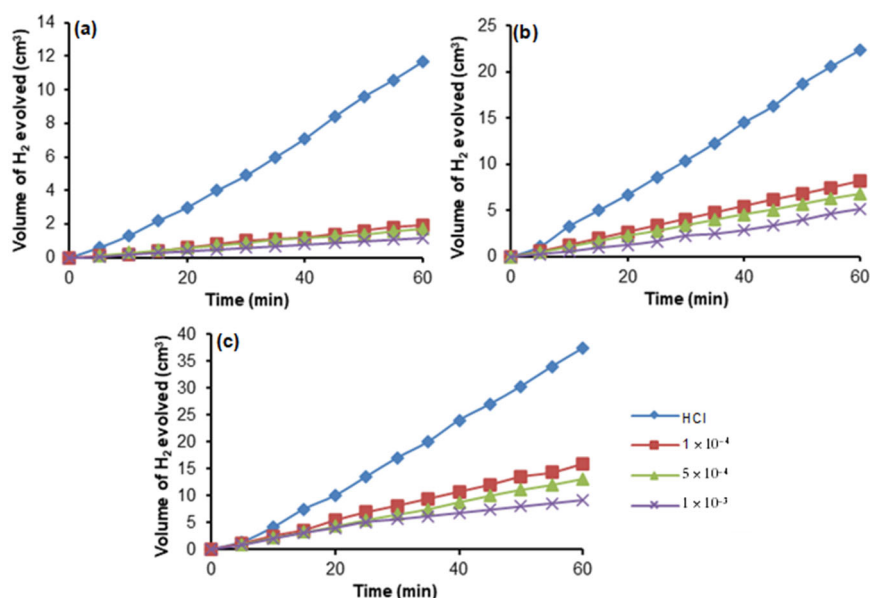


Fig 3. Hydrogen gas evolved (cm³) with time (min) for the corrosion of carbon steel in 1 M HCl at (a) 308, (b) 318, and (c) 328 K in the presence and absence of SSZ

Adsorption Isotherm

Various mathematical models were evaluated to identify the most accurate representation of the adsorption isotherms. Eq. (3) describes the Langmuir adsorption isotherm that the corrosion inhibition system under inquiry complies with [24].

$$\frac{C}{\theta} = \frac{1}{K_{\text{ads}}} + C \quad (3)$$

The experiment involved plotting the ratio of the inhibitor concentration (C) to θ against the inhibitor concentration. The resulting graph displayed a straight line (Fig. 4) with a slope close to 0.9997 and a regression coefficient of approximately 0.9923. These findings indicate that the adsorption of inhibitors follows a uniform monolayer Langmuir model, suggesting no interaction with adjacent sites. The high correlation observed in accordance with the Langmuir adsorption isotherm further strengthens the validity of this approach [25-26].

Table 3 provides the values for the adsorptive equilibrium constant (K_{ads}), which highlights that higher values correspond to robust adsorption of the produced inhibitor onto the CS surface in 1 M HCl at elevated

temperatures. This strong adsorption can be attributed to the creation of coordinated bonds between the synthesized inhibitor and the d-orbital of iron located on the CS surface.

Thermodynamic Parameters

K_{ads} can be computed from the intercept of Eq. (3) (Table 3). Eq. (4) can be utilized to compute the free energy of adsorption based on K_{ads} .

$$\Delta G^{\circ}_{\text{ads}} = -RT \ln(55.5 K_{\text{ads}}) \quad (4)$$

The given statement suggests that the calculated value of ΔG° falls within the range of -36.748 to -38.377 kJ mol $^{-1}$. In this equation, R represents the gas constant, T represents the absolute temperature of the experiment, and 55.5 represents the concentration of water in solution in mol dm $^{-3}$. A negative free energy implies that the process of adsorption of the inhibitor onto the metal surface is spontaneous. If the magnitude of ΔG° is approximately -20 kJ mol $^{-1}$ or less negative, the interaction between the inhibitor and the charged metal surface is primarily electrostatic or physical in nature. Chemisorption refers to a type of bond formation that occurs when the energy is approximately

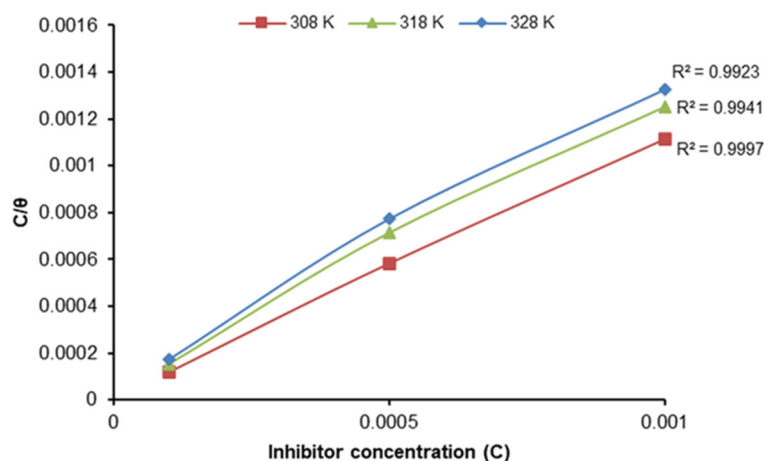


Fig 4. Carbon steel Langmuir adsorption plots in 1 M HCl at different temperatures with varying amounts of SSZ

Table 3. Thermodynamic parameters for the adsorption of SSZ on CS in 1 M HCl at different temperatures from the Langmuir adsorption isotherm

T (K)	slope	R ²	log K _{ads}	ΔG ^o _{ads} (kJ mol ⁻¹)	ΔH ^o _{ads} (kJ mol ⁻¹)	ΔS ^o _{ads} (kJ mol ⁻¹)
308	0.9054	0.9997	4.764	-38.377		-0.0853
318	0.8160	0.9941	4.247	-36.463	-64.640	-0.0886
328	0.7801	0.9923	4.102	-36.748		-0.0850

-40 kJ mol^{-1} or more negative. In the current study, the obtained energy values ranged from -20 to -40 kJ mol^{-1} . This suggests that the interaction observed in all three cases is a combination of physisorption (weaker, nonchemical interaction) and chemisorption. As a result, the interaction can be described as complex. The heat of adsorption (ΔH_{ads}) can be calculated using the vant' Hoff equation (Eq. (5)) [27].

$$\log K_{\text{ads}} = (-\Delta H_{\text{ads}}/2.303 RT) + \text{constant} \quad (5)$$

By plotting $\log K_{\text{ads}}$ versus $1/T$, a straight line with a slope of $-\Delta H_{\text{ads}}/2.303 R$ was obtained (Fig. 5). According to Table 3, all the thermodynamic parameters are provided. The positive value of the adsorption entropy suggested that the solvent's entropy was more dominant than that of the solute in the inhibitor. In a study by Bentiss et al. [28], if the ΔH° is greater than 0, the adsorption process is considered chemisorption. Conversely, if ΔH° is less than 0, it could be either physisorption or chemisorption. Additionally, for an exothermic process, the magnitude of ΔH° can help differentiate between physisorption and chemisorption [26]. During physisorption, the enthalpy of adsorption typically falls below 40 kJ mol^{-1} , whereas during chemisorption, it exceeds 100 kJ mol^{-1} [27]. The results obtained indicate that the investigated compound exhibits a small, negative enthalpy of adsorption ($-64.640 \text{ kJ mol}^{-1}$), indicating physisorption. Eq. (6) is used to calculate the adsorption entropy [29].

$$\Delta G^\circ_{\text{ads}} = \Delta H^\circ_{\text{ads}} - T\Delta S^\circ_{\text{ads}} \quad (6)$$

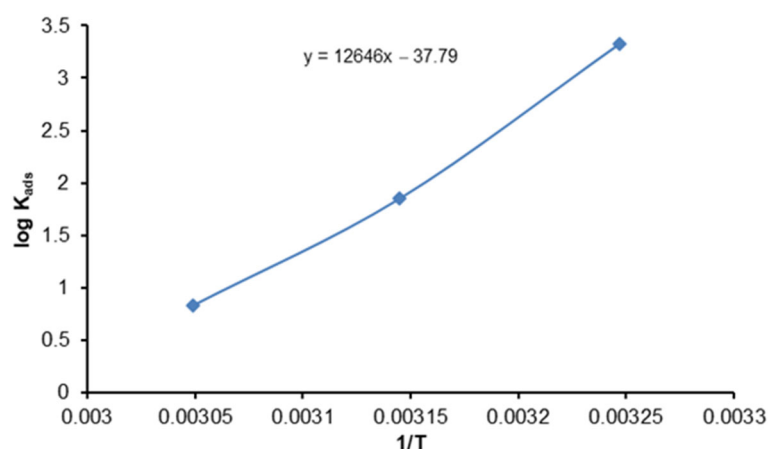


Fig 5. The correlation between the logarithm of the adsorption equilibrium constant ($\log K_{\text{ads}}$) and the reciprocal temperature ($1/T$) for CS immersed in a 1 M HCl solution with varying concentrations of inhibitors

Quantum Chemical Calculations


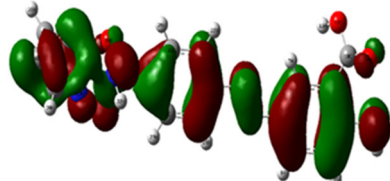
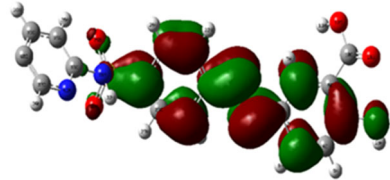
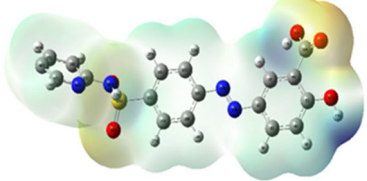
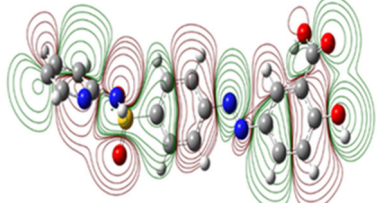
The computations were conducted using the Gaussian 09 software package. Full geometry optimizations were performed using density function theory (DFT) with B3LYP and the 6-31G (d) basis set [30]. Quantum chemical calculations have conclusively demonstrated their marked effectiveness as a tool for studying the mechanism of corrosion inhibition [31–34]. One of the main uses of quantum chemical calculation methods is to explain trends in experimental results, particularly when it is rare to obtain such information directly from experimental data [35]. The observed molecular attributes are many and noteworthy, as Table 4 demonstrates. These characteristics include the dipole moment, ionization potential, hardness, softness, electron affinity, electronegativity, and the energy levels of LUMO (E_{LUMO}) and HOMO (E_{HOMO}). Furthermore, the optimum geometrical configurations of SSZ are shown in Table 5. It's interesting to note that both sides of the molecule under study have a large distribution of the lowest LUMO and HOMO.

The metal surface is effectively bonded with the inhibitor through interactions between the lone pair of electrons on the heteroatoms and the vacant orbitals on the iron atom. The chemical species adsorption and reactivity are significantly affected by the HOMO and LUMO frontier orbitals. The tendency of a molecule to donate electrons to acceptor molecules with low-energy empty molecular orbitals increases as the value of E_{HOMO}

Table 4. List of quantum chemical parameters for SSZ

Quantum chemical parameters	GA
Total Energy (kJ mol ⁻¹)	-4428842000
Dipole moment (Debye's)	3.698600000
E _{HOMO} (eV)	-4.915231308
E _{LUMO} (eV)	-2.833543908
$\Delta E_{\text{gap}} = E_{\text{LUMO}} - E_{\text{HOMO}}$ (eV)	2.081687400
Ionization potential, I = -E _{HOMO}	4.915231308
Electron affinity, A = -E _{LUMO}	2.833543908
Electronegativity, $\chi = -\frac{1}{2}(E_{\text{HOMO}} + E_{\text{LUMO}})$	3.874387608
Hardness, $\eta = \Delta E_{\text{gap}}/2$	1.040843700
Softness, $\sigma = 1/\eta$	0.960759046
Chemical potential, $\mu = -\frac{1}{2}(I + A)$	-3.874387608
Number of transferred electrons, $\Delta N = [\chi_{\text{Fe}} - \chi_{\text{inh}}]/[2(\eta_{\text{Fe}} + \eta_{\text{inh}})]$	1.501480190
Solvation energy (SE), kJ mol ⁻¹	-104.3907999
%IE = 123.418 - 9.334 (D.M) - 0.131 (SE)	75.22000000

Table 5. Optimized geometrical configuration structures of the SSZ

Quantum chemical structure	GA
Optimized geometry	
HOMO	
LUMO	
ESP	
Electrostatic potential map	

increases, resulting in greater inhibition efficiency. Similarly, when the value of E_{LUMO} is lower, the molecule is more likely to accept electrons, making it an efficient inhibitor [36-37]. The molecule under examination SSZ possesses an energy level of -4.92 eV, indicating its ability to readily donate electrons. As a result, the inhibitor demonstrated a lower value of ΔE_{gap} , indicating its efficacy. As a result, the inhibitor has a lower ΔE_{gap} value. According to the boundary of molecular orbitals theory of chemical reactions, the formation of the transition state is attributed to the interaction between the HOMO and the LUMO of the species involved [38]. Consequently, the inhibitor can effectively interact with the CS surface. It is widely recognized that a higher dipole moment will enhance the inhibition of corrosion [39-40]. The higher efficiency of the inhibitors is due to the tendency of Fe, a soft acid, to preferentially react with soft bases such as SSZ, which have low hardness and high softness. This observation is strongly supported by the excellent agreement between the results obtained from quantum chemical calculations and the experimental findings.

As was previously indicated, descriptions of the electrical and physical-chemical parameters that affect the efficiency of inhibition have been given. These properties are essential for understanding how effective molecules are at inhibiting corrosion. It is crucial to remember that there isn't a clear-cut connection between these traits and the effectiveness of corrosion inhibition. Because the wide range of chemical parameters affects molecule efficiency, it is difficult to create a direct link that validates the intricate nature of interactions involved in the inhibitory processes. However, Eq. (7) can still be used to get the theoretical inhibitory efficiency [31,39,41].

$$IE_{Theor} = 123.418 - 9.334 \times D.M - 0.131 \times (SE) \quad (7)$$

where SE is the solvation energy that the Firefly Program computes [41] and D.M. is dipole moment.

Inhibition Mechanism

Based on the computational results of the SSZ inhibitors, it is likely that the adsorption mechanism of SSZ on mild steel involves various types of interactions. One possible interaction is through chemisorption, where the vacant d-orbital of iron (Fe) interacts with the atoms of oxygen (O), sulfur (S), and nitrogen (N) in SSZ, forming

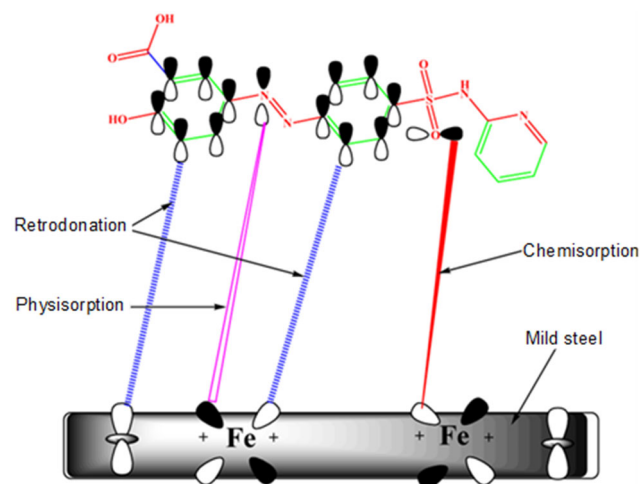


Fig 6. Proposed inhibition mechanism of (SSZ)

a strong bond [42-43]. This interaction helps protect mild steel from corrosion by sharing lone-pair electrons. Additionally, a retro-donation interaction occurs between the ionized Fe atoms on the steel surface and the π -electrons of the aromatic ring in SSZ [44-45]. This interaction further contributes to the inhibition of corrosion. The adsorbed SSZ also covers a large surface area, forming a protective film over the steel surface, which enhances the inhibition performance Fig. 6.

CONCLUSION

SSZ effectively inhibited CS corrosion (89.74%) in 1 M HCl solution as an aggressive medium and 1.0×10^{-3} M of SSZ at 308 K by using the hydrogen evolution method. Experimental and theoretical calculations showed that the anti-corrosion efficiency correlated directly with increasing the inhibitor SSZ concentration. Also, these calculations showed the investigated SSZ acted as a mixed-type inhibitor. The determination of various thermodynamic parameters and investigation of the adsorption isotherm demonstrate that the adsorption follows the Langmuir model and is classified as physisorption. The quantitative chemical parameters and full geometry optimizations were calculated using DFT. The quantum chemical methods show very good agreement with the experimental results.

ACKNOWLEDGMENTS

The authors are grateful to Al-Shatrah University and Uruk University for technical support.

■ CONFLICT OF INTEREST

The authors declare no conflict of interest.

■ AUTHOR CONTRIBUTIONS

Hadi Thamer Obaid, Muthanna Mahmood Mutar and Safaa Hussein Ali contributed to the conception and design of the study. Hadi Thamer Obaid performed the experimental part and wrote the first draft. Muthanna Mahmood Mutar performed a computational simulation and wrote the first draft. Safaa Hussein Ali revised and edited the final draft. All authors read and approved the final version of this manuscript.

■ REFERENCES

- [1] Khalib, A.A.K., Al-Hazam, H.A.J., and Hassan, A.F., 2022, Inhibition of carbon steel corrosion by some new organic 2-hydroselenoacetamide derivatives in HCl medium, *Indones. J. Chem.*, 22 (5), 1269–1281.
- [2] Salleh, N.I.H., and Abdullah, A., 2019, Corrosion inhibition of carbon steel using palm oil leaves extract, *Indones. J. Chem.*, 19 (3), 747–752.
- [3] Baari, M.J., and Pratiwi, R.Y., 2022, Application of carbon dots as corrosion inhibitor: A systematic literature review, *Indones. J. Chem.*, 22 (5), 1427–1453.
- [4] Baari, M.J., and Sabandar, C.W., 2021, A Review on expired drug-based corrosion inhibitors: Chemical composition, structural effects, inhibition mechanism, current challenges, and future prospects, *Indones. J. Chem.*, 21 (5), 1316–1336.
- [5] El Assiri, E.H., Driouch, M., Bensouda, Z., Beniken, M., Elhaloui, A., Sfaira, M., and Saffaj, T., 2019, Computational study and QSPR approach on the relationship between corrosion inhibition efficiency and molecular electronic properties of some benzodiazepine derivatives on C-steel surface, *Anal. Bioanal. Electrochem.*, 11 (3), 373–395.
- [6] Ali, S.H., Abd Alredha, H.M., and Abdulhussein, H.S., 2020, Antibiotic activity of new species of Schiff base metal complexes, *Period. Tche Quim.*, 17 (35), 837–859.
- [7] Bensouda, Z., Ellassiri, E., Galai, M., Sfaira, M., Farah, A., and Ebn Touhami, M., 2018, Corrosion inhibition of mild steel in 1 M HCl solution by *Artemisia abrotanum* essential oil as an eco-friendly inhibitor, *J. Mater. Environ. Sci.*, 9 (6), 1851–1865.
- [8] Beniken, M., Driouch, M., Sfaira, M., Hammouti, B., Ebn Touhami, M., and Mohsin, M.A., 2018, Anti-corrosion activity of a polyacrylamide with high molecular weight on C-steel in acidic media: Part 1, *J. Bio- Tribo-Corros.*, 4 (3), 38.
- [9] Beniken, M., Driouch, M., Sfaira, M., Hammouti, B., Ebn Touhami, M., and Mohsin, M., 2018, Kinetic–thermodynamic properties of a polyacrylamide on corrosion inhibition for C-steel in 1.0 M HCl medium: Part 2, *J. Bio- Tribo-Corros.*, 4 (3), 34.
- [10] Bensouda, Z., Driouch, M., Belakhmima, R.A., Sfaira, M., Ebn Touhami, M., and Farah, A., 2018, *Thymus sahraouian* essential oil as corrosion eco-friendly inhibitor for mild steel in a molar hydrochloric acid solution, *Port. Electrochim. Acta*, 36 (5), 339–364.
- [11] Bensouda, Z., Driouch, M., Sfaira, M., Farah, A., Ebn Touhami, M., Hammouti, B., and Emran, K.M., 2018, Effect of *Mentha piperita* essential oil on mild steel corrosion in hydrochloric acid, *Int. J. Electrochem. Sci.*, 13 (8), 8198–8221.
- [12] Khan, M.A.A., Irfan, O.M., Djavanroodi, F., and Asad, M., 2022, Development of sustainable inhibitors for corrosion control, *Sustainability*, 14 (15), 9502.
- [13] Verma, C., Ebenso, E.E., Quraishi, M.A., and Hussain, C.M., 2021, Recent developments in sustainable corrosion inhibitors: Design, performance and industrial scale applications, *Mater. Adv.*, 2 (12), 3806–3850.
- [14] Mohsenifar, F., Jafari, H., and Sayin, K., 2016, Investigation of thermodynamic parameters for steel corrosion in acidic solution in the presence of *N,N*-bis(phloroacetophenone)-1,2 propanediamine, *J. Bio- Tribo-Corros.*, 2 (1), 1.
- [15] Ganapathi Sundaram, R., and Sundaravadivelu, M., 2016, Anti-corrosion activity of 8-quinoline sulphonyl chloride on mild steel in 1 M HCl solution, *J. Metall.*, 2016 (1), 8095206.
- [16] Al-Amiery, A.A., Wan Isahak, W.N.R., and Al-Azzawi, W.K., 2023, Corrosion inhibitors: Natural

- and synthetic organic inhibitors, *Lubricants*, 11 (4), 174.
- [17] Aslam, R., Serdaroglu, G., Zehra, S., Kumar Verma, D., Aslam, J., Guo, L., and Quraishi, M.A., 2022, Corrosion inhibition of steel using different families of organic compounds: Past and present progress, *J. Mol. Liq.*, 348, 118373.
- [18] Wazzan, N., and Al-Mhyawi, S., 2017, Application of newly quiniline-3-carbonitriles as corrosion inhibitors on mild steel in 1.0 M HCl: Electrochemical measurements, HF and DFT/B3LYP calculations, *Int. J. Electrochem. Sci.*, 12 (10), 9812–9828.
- [19] Abdel Hameed, R.S., 2019, Schiff bases as corrosion inhibitor for aluminum alloy in hydrochloric acid medium, *Tenside, Surfactants, Deterg.*, 56 (3), 209–215.
- [20] Berrissoul, A., Dafali, A., Cherrak, K., Romane, A., Ouarhach, A., Guenbour, A., and Zarrouk, A., 2019, A comparative study on the corrosion behavior of mild steel and aluminum alloy in acidic medium using green corrosion inhibitor, *Phys. Sci.*, 14 (3), 19–31.
- [21] Sarigul, M., Deveci, P., Kose, M., Arslan, U., Türk Dagi, H., and Kurtoglu, M., 2015, New tridentate azo–azomethines and their copper(II) complexes: Synthesis, solvent effect on tautomerism, electrochemical and biological studies, *J. Mol. Struct.*, 1096, 64–73.
- [22] Shetty, P., 2020, Schiff bases: An overview of their corrosion inhibition activity in acid media against mild steel, *Chem. Eng. Commun.*, 207 (7), 985–1029.
- [23] Madkour, L.H., and Elroby, S.K., 2015, Inhibitive properties, thermodynamic, kinetics and quantum chemical calculations of polydentate Schiff base compounds as corrosion inhibitors for iron in acidic and alkaline media, *Int. J. Ind. Chem.*, 6 (3), 165–184.
- [24] Obaid, H.T., Kadhum, M.Y., and Abdulnabi, A.S., 2022, Quantum chemical calculations and experimental studies of using azo dye as corrosion inhibitors for on carbon steel in acidic medium, *ACE J. Adv. Res. Chem. Sci.*, 2 (1), 1–9.
- [25] Li, L., Liu, W., Qi, F., Wu, D., and Zhang, Z., 2022, Effects of deformation twins on microstructure evolution, mechanical properties and corrosion behaviors in magnesium alloys - A review, *J. Magnesium Alloys*, 10 (9), 2334–2353.
- [26] Abakedi, O.U., 2017, *Solenostemon monostachyus* leaf extract as eco-friendly inhibitor of aluminium corrosion in acidic medium, *Asian J. Chem. Sci.*, 2 (1), 1–9.
- [27] Saranya, J., Sowmiya, M., Sounthari, P., Parameswari, K., Chitra, S., and Senthilkumar, K., 2016, N-heterocycles as corrosion inhibitors for mild steel in acid medium, *J. Mol. Liq.*, 216, 42–52.
- [28] Bentiss, F., Traisnel, M., and Lagrenee, M., 2000, The substituted 1,3,4-oxadiazoles: A new class of corrosion inhibitors of mild steel in acidic media, *Corros. Sci.*, 42 (1), 127–146.
- [29] Hamani, H., Douadi, T., Al-Noaimi, M., Issaadi, S., Daoud, D., and Chafaa, S., 2014, Electrochemical and quantum chemical studies of some azomethine compounds as corrosion inhibitors for mild steel in 1 M hydrochloric acid, *Corros. Sci.*, 88, 234–245.
- [30] Loto, R.T., Loto, C.A., Popoola, A.P., and Fedotova, T., 2016, Electrochemical studies of the inhibition effect of 2-dimethylaminoethanol on the corrosion of austenitic stainless steel type 304 in dilute hydrochloric acid, *Silicon*, 8 (1), 145–158.
- [31] Douadi, T., Hamani, H., Daoud, D., Al-Noaimi, M., and Chafaa, S., 2017, Effect of temperature and hydrodynamic conditions on corrosion inhibition of an azomethine compounds for mild steel in 1 M HCl solution, *J. Taiwan Inst. Chem. Eng.*, 71, 388–404.
- [32] Guo, L., Zhu, S., Zhang, S., He, Q., and Li, W., 2014, Theoretical studies of three triazole derivatives as corrosion inhibitors for mild steel in acidic medium, *Corros. Sci.*, 87, 366–375.
- [33] Chaouiki, A., Lgaz, H., Salghi, R., Gaonkar, S.L., Bhat, K.S., Jodeh, S., Toumiat, K., and Oudda, H., 2019, New benzohydrazide derivative as corrosion inhibitor for carbon steel in a 1.0 M HCl solution: Electrochemical, DFT and Monte Carlo simulation studies, *Port. Electrochim. Acta*, 37 (3), 147–165.

- [34] Akin, M., Günşel, A., Bilgiçli, A.T., Tüzün, B., Arabaci, G., Şaki, N., and Yarasir, M.N., 2020, The water-soluble peripheral substituted phthalocyanines as corrosion inhibitors for copper in 0.1 N HCl: Gravimetric, electrochemical, SEM-EDS, and quantum chemical calculations, *Prot. Met. Phys. Chem. Surf.*, 56 (3), 609–618.
- [35] Abdelshafi, N.S., Sadik, M.A., Shoeib, M.A., and Halim, S.A., 2022, Corrosion inhibition of aluminum in 1 M HCl by novel pyrimidine derivatives, EFM measurements, DFT calculations and MD simulation, *Arabian J. Chem.*, 15 (1), 103459.
- [36] Fouda, A.E.A.S., Etaiw, S.E.H., Ismail, M.A., Abd El-Aziz, D.M., and Eladl, M.M., 2022, Novel naphthybithiophene derivatives as corrosion inhibitors for carbon steel in 1 M HCl: Electrochemical, surface characterization and computational approaches, *J. Mol. Liq.*, 367, 120394.
- [37] Ma, Q., Qi, S., He, X., Tang, Y., and Lu, G., 2017, 1,2,3-Triazole derivatives as corrosion inhibitors for mild steel in acidic medium: Experimental and computational chemistry studies, *Corros. Sci.*, 129, 91–101.
- [38] Verma, C., Saji, V.S., Quraishi, M.A., and Ebenso, E.E., 2020, Pyrazole derivatives as environmental benign acid corrosion inhibitors for mild steel: Experimental and computational studies, *J. Mol. Liq.*, 298, 111943.
- [39] Zakaria, K., Negm, N.A., Khamis, E.A., and Badr, E.A., 2016, Electrochemical and quantum chemical studies on carbon steel corrosion protection in 1 M H₂SO₄ using new eco-friendly Schiff base metal complexes, *J. Taiwan Inst. Chem. Eng.*, 61, 316–326.
- [40] Du, L., Zhao, H., Hu, H., Zhang, X., Ji, L., Li, H., Yang, H., Li, X., Shi, S., Li, R., Tang, X., and Yang, J., 2014, Quantum chemical and molecular dynamics studies of imidazoline derivatives as corrosion inhibitor and quantitative structure–activity relationship (QSAR) analysis using the support vector machine (SVM) method, *J. Theor. Comput. Chem.*, 13 (2), 1450012.
- [41] Fouda, A.S., El-Hallag, I.S., El-Barbary, A.A., and El Salamony, F.M., 2023, Novel 1,2,4-triazole derivatives as corrosion inhibitors for copper in HNO₃ solution, *Egypt. J. Chem.*, 66 (4), 291–303.
- [42] Méndez, C.M., Gervasi, C.A., Pozzi, G., and Ares, A.E., 2023, Corrosion inhibition of aluminum in acidic solution by *Ilex paraguariensis* (yerba mate) extract as a green inhibitor, *Coatings*, 13 (2), 434.
- [43] Obaid, H.T., Kadhum, M.Y., and Abdalnabi, A.S., 2022, Azo Schiff base derived from 2-hydroxy-1-naphthaldehyde as corrosion inhibitors for carbon steel in HCl medium: Experimental and theoretical studies, *Mater. Today: Proc.*, 60, 1394–1401.
- [44] Alamiery, A.A., 2021, Anti-corrosion effect of thiosemicarbazide derivative on mild steel in 1 M hydrochloric acid and 0.5 M sulfuric acid: Gravimetric and theoretical studies, *Mater. Sci. Energy Technol.*, 4, 263–273.
- [45] Gozem, S., Huntress, M., Schapiro, I., Lindh, R., Granovsky, A.A., Angeli, C., and Olivucci, M., 2012, Dynamic electron correlation effects on the ground state potential energy surface of a retinal chromophore model, *J. Chem. Theory Comput.*, 8 (11), 4069–4080.